HHS Public Access

Author manuscript

Nano Lett. Author manuscript; available in PMC 2024 September 08.

Published in final edited form as:

Nano Lett. 2024 July 31; 24(30): 9163–9168. doi:10.1021/acs.nanolett.4c01094.

High-Verdet Constant and Low-Optical Loss Tb^{3+} Doped Magnetite Nanoparticles

Jan Bartos[§],
Department of Electrical, Computer, and Energy Engineering, University of Colorado Boulder, Boulder, Colorado 80309, United States

Taleb Ba Tis[§],
Material Science and Engineering Program, University of Colorado Boulder, Boulder, Colorado 80309, United States

Mingming Nie,
Department of Electrical, Computer, and Energy Engineering, University of Colorado Boulder, Boulder, Colorado 80309, United States

Shu-Wei Huang,
Department of Electrical, Computer, and Energy Engineering, University of Colorado Boulder, Boulder, Colorado 80309, United States

Wounjhang Park
Department of Electrical, Computer, and Energy Engineering and Material Science and Engineering Program, University of Colorado Boulder, Boulder, Colorado 80309, United States

Abstract

Magneto-optical (MO) polymer nanocomposites have emerged as alternatives to conventional MO crystals, particularly in nanophotonics applications, thanks to their better processing flexibility and superior Verdet constants. However, a higher Verdet constant commonly comes with excessive optical loss due to increased absorption and scattering, resulting in a constant or reduced figure-of-merit (FOM) defined as the Verdet constant over optical loss. By doping magnetite (Fe_3O_4) nanoparticles with Tb^{3+} ions, we report a new strategy to enhance the Verdet constant without increasing the optical loss. The Fe_3O_4:Tb^{3+} nanocomposite is one of a kind that simultaneously achieves a state-of-the-art Verdet constant of 5.6×10^5 °/T·m and a state-of-the-art FOM of 31°/T in the near-infrared region.

Corresponding Authors: Wounjhang Park – Department of Electrical, Computer, and Energy Engineering and Material Science and Engineering Program, University of Colorado Boulder, Boulder, Colorado 80309, United States; won.park@colorado.edu, **Shu-Wei Huang** – Department of Electrical, Computer, and Energy Engineering, University of Colorado Boulder, Boulder, Colorado 80309, United States; ShuWei.Huang@colorado.edu.

[§]J.B. and T.B.T. contributed equally.

Supporting Information

The Supporting Information is available free of charge at https://pubs.acs.org/doi/10.1021/acs.nanolett.4c01094.
Terbium-doped nanoparticle fabrication, material characterization, and optical setup details (PDF)

The authors declare no competing financial interest.

Complete contact information is available at: https://pubs.acs.org/10.1021/acs.nanolett.4c01094

Graphical Abstract

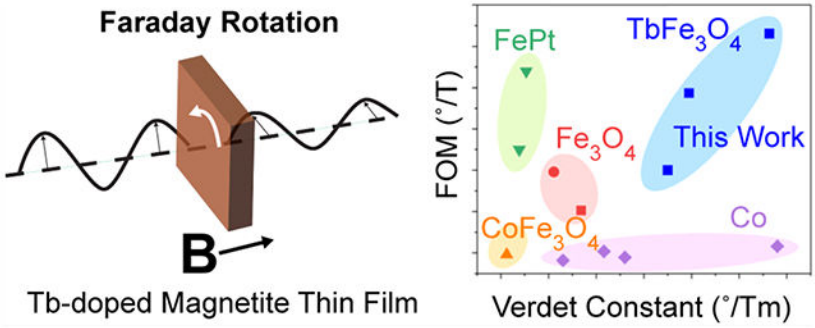

Keywords

Nanoparticles; Faraday Rotation; Verdet Constant; Magnetite; Nanocomposites; Magnetometer; Rare Earth Doping; Polymer; PMMA

The Faraday effect has been used in a wide range of applications in lasers, telecommunications, materials science, quantum computing, and remote sensing.[1–4] It describes the polarization rotation that linearly polarized light undergoes when passing through a magneto-optical (MO) medium.[5,6] Traditionally, MO garnet crystals such as terbium gallium garnet (TGG), terbium aluminum garnets (TAG), yttrium iron garnet (YIG), and rare-earth doped glasses have used Faraday rotators due to their high transparency.[3,4] To compensate for the rather weak to moderate Faraday effect, these materials are commonly used in bulk configuration with mm to m thicknesses including optical fiber materials.[7,8] In recent years, MO polymer nanocomposites have been introduced as alternatives to the conventional MO crystal.[3,9–15] Thanks to their magnetic nanoparticle content, these polymer nanocomposites exhibit ultrahigh MO responsivities and thus can achieve large Faraday rotation with submillimeter interaction lengths. Additionally, they are more flexible for fabrication and processing compared to single crystals,[3,16,17] enabling MO polymer nanocomposite thin film that can be integrated with microfabricated devices for various photonic and magnetic applications.

The major drawback of MO polymer nanocomposites is their high optical loss stemming from nanoparticle's intrinsic material absorption and aggregation induced scattering.[3,9,13] The trade-off between MO responsivity and optical loss can be quantified by defining an MO figure-of-merit: FOM = V/α where V is a measure of the MO responsivity known as the Verdet constant and α is the attenuation coefficient.[15] While the Verdet constant is a useful parameter quantifying MO device performance in a power-abundant regime, FOM is a better metric for applications in the power-starved regime, when device insertion loss cannot be tolerated.

To mitigate the scattering losses, the nanoparticles are often coated with polymerizable ligands which allow them to be anchored to the polymer matrix during the polymerization reaction, and thus maintain their spatial dispersion.[9,18,19] Other strategies to reduce the scattering loss also include lowering nanoparticle concentration,[9] using block copolymers,[15]

and employing multistep spin-coating methods with intervening spacer layers.[9,13] These strategies have been proven to be very effective, leaving the fundamental trade-off between the MO responsivity and absorption coefficient the remaining challenge to be addressed.[6]

In this work, we report a new strategy to enhance both the Verdet constant and the FOM of magnetite (Fe_3O_4) nanoparticles via doping with terbium (Tb^{3+}) ions. To induce a strong MO response far away from absorption peaks, it has been suggested that materials containing ions with a C-term Faraday response, which arises from the Zeeman splitting of ground state due to external magnetic field, should be used.[6] Tb^{3+} ions present an ideal candidate for examining this hypothesis. They possess a high magnetic moment, strong spin–orbit coupling, and have allowed optical transitions far from the near-infrared (NIR) region.[20] Earlier studies have investigated the impact of Tb^{3+} and other rare-earth dopants on the magnetic properties of magnetite nanoparticles such as saturation magnetization, coercivity, magnetic moment, and relaxivity.[21–26] The few articles that discussed the effect of rare-earth doping on the magneto-optical properties were either limited in their scope, analysis, and data presentation or have been carried out on other ferrite systems such as cobalt ferrite.[27,28] Thus, the effect that Tb^{3+} and other rare ion doping might have on the Faraday effect of magnetite nanoparticles remains largely unexplored.

By embedding Fe_3O_4:Tb^{3+} nanoparticles in a poly(methyl methacrylate) (PMMA) matrix, the Verdet constants and FOM at 980 nm were characterized as a function of the Tb^{3+} doping. We show that an optimal Tb^{3+} doping density of 1.12 mol % results in a 3-fold enhancement of both the Verdet constant and the FOM compared to undoped nanoparticles. The PMMA-Fe_3O_4:Tb^{3+} nanocomposite is one of a kind that simultaneously achieves a high Verdet constant of 5.6×10^5 °/T·m and a high FOM of 31°/T in the NIR, benefiting all applications in either the power-abundant or the power-starved regimes.

Six nanoparticle batches were prepared with increasing amounts of Tb^{3+} using the process described in detail in the Supporting Information (SI). As shown in Figure 1(A–G), the nanoparticles were roughly 14–16 nm in size with standard deviations of around 2 nm. Previous reports on the size dependence of the Faraday effect have shown that larger nanoparticles tend to exhibit stronger MO response.[14,29,30] The gain in MO responsivity can, however, be undermined by the propensity of larger nanoparticle to aggregate due to their strong magnetic interactions.[10,31] Thus, there is an optimal size where the MO responsivity can be maximized without causing severe aggregation. We opted for 14–16 nm sized nanoparticles because that is the range where both the Verdet constant and FOM were maximized for our system as shown in Figure S2. The Tb^{3+} doping density in the nanoparticles was determined via inductively coupled plasma mass spectrometry (ICP-MS) analysis as shown in Figure 1(H) and further discussed in the SI.

Following the synthesis, the Fe_3O_4:Tb^{3+} nanoparticles were embedded into a PMMA matrix by using an *in situ* free-radical polymerization reaction. To ensure excellent dispersion in the polymer matrix, the nanoparticles were first functionalized with the polymerizable ligand, bis(2-methacryloyloxy)-ethylphosphate (BMEP). The BMEP-functionalized nanoparticles were then mixed with the methyl methacrylate (MMA) monomers and the initiator. The subsequent polymerization reaction produces the desired

PMMA-Fe_3O_4:Tb^{3+} nanocomposite with a loading of 4 wt %. Details of surface functionalization and polymerization processes are provided in SI.

Figure 2(A) shows the wavelength dependent absorption spectrum of the PMMA-Fe_3O_4:Tb^{3+} nanocomposite films measured with VIS–NIR spectrophotometry. The intervalence charge transfer (IVCT) transitions of the Fe^{3+} and Fe^{2+} ions[32,33] that result in magnetite's strong MO response also led to a strong UV absorption band and an elevated NIR absorption peak centered around 1400 nm. On the other hand, no additional NIR absorption is observed when Tb^{3+} is doped into the magnetite nanoparticles, rendering Tb^{3+} doping an effective strategy to simultaneously enhance the Verdet constant and FOM. The lack of any significant changes in the absorption spectra after doping are likely due to the low Tb^{3+} concentration and its small absorption cross-section in comparison to magnetite.[32,34] The 15% variation in absorption coefficients among different samples is attributed to the uncertainty of the nanoparticle loading, which is uncorrelated with the Tb^{3+} doping density. Inset of Figure 2(A) shows an optical image of representative 30-μm thick nanocomposite films with different Tb^{3+} doping densities. The text behind the PMMA-Fe_3O_4:Tb^{3+} nanocomposite films remains sharp without distortion, confirming that the Tb^{3+} doping does not degrade the optical quality of the nanocomposite films.

The Verdet constant measurement apparatus, illustrated in Figure 2(B), was designed following the setup reported in Pavlopoulos et al.[9] A more detailed description including information about calibration can be found in SI. Briefly, we measure the Faraday rotation of the PMMA-Fe_3O_4:Tb^{3+} nanocomposite films as a function of the applied DC magnetic fields. The Faraday rotation, θ_F, is then normalized by the film thickness, L, to determine the Verdet constant, according to the equation:

$$\theta_F / L = V B \tag{1}$$

where V is the Verdet constant, B is the applied DC magnetic field, and θ_F / L is the specific Faraday rotation. When the applied DC magnetic field is plotted against the specific Faraday rotation, the slope of the response is determined by the Verdet constant.

It is important to note that while eq 1 assumes a linear relationship between the Faraday rotation and magnetic field, some MO materials deviate from the linear behavior especially at high magnetic fields.[3,10] To find the validity range of eq 1 for our material, we first measured the Faraday rotation of the undoped nanoparticle over a wide range of magnetic fields (i.e., 0–90 mT). As shown in Figure 3(A), the Faraday rotation starts saturating at magnetic fields greater than 10 mT. As a result, we used magnetic fields below 0.5 mT, safely within the linear region, as shown in Figure 3(B) for all subsequent Faraday rotation measurements.

Figure 4(A) shows the Verdet constants and FOMs of the PMMA-Fe_3O_4:Tb^{3+} nanocomposite films as a function of Tb^{3+} doping. Both Verdet constants and FOMs reach their peaks at 1.12 mol % Tb^{3+} doping, confirming the effectiveness of Tb^{3+} doping to simultaneously enhance the Verdet constant and FOM. The maximum Verdet constant and

FOM are 5.6×10^5 °/T·m and 31°/T, respectively, representing a 3-fold enhancement over the undoped magnetite nanoparticles. Figure 4(B) compares our results to other room temperature MO polymer nanocomposites with 4 wt % loading in the NIR. Our new PMMA-Fe_3O_4:Tb^{3+} nanocomposite is one of a kind that achieves not only high Verdet constant but also high FOM. Compared to the best Co nanocomposite that has a comparable Verdet constant, our new PMMA-Fe_3O_4:Tb^{3+} nanocomposite exhibits an over 5-fold higher FOM. Compared to the best FePt-nanocomposite that has a comparable FOM, our new PMMA-Fe_3O_4:Tb^{3+} nanocomposite exhibits an order-of-magnitude higher Verdet constant. Our new PMMA-Fe_3O_4:Tb^{3+} nanocomposite outperforms other MO polymer nanocomposites in both Verdet constant and FOM.

Magnetite's strong MO response has been attributed to the allowed IVCT transitions of the Fe^{3+} and Fe^{2+} ions.[33] The paramagnetic line shape of these IVCT transitions, particularly in the UV and NIR region, suggest that their contribution to Faraday rotation is of a C-term nature. The magnitude of the C-term MO response is proportional to the dipole transition strength and the magnetic moment of the ground state as shown in eq 2:

$$C(j \leftarrow n) = \frac{1}{d_g}\langle n|m_Z|n\rangle \mathrm{Im}\{\langle n|\mu_x|j\rangle\langle j|\mu_y|n\rangle\} \quad (2)$$

where n and j are the initial and final states, d_g is the degeneracy of the initial state, the $\langle n|m_Z|n\rangle$ term is related to the ground state magnetic moment and the $\mathrm{Im}\{\langle n|\mu_x|j\rangle\langle j|\mu_y|n\rangle\}$ is related to the dipole transition strength, m_Z is the magnetic dipole moment operator parallel to the light propagation direction, and μ_x and μ_y are electric dipole moment operators perpendicular to the light propagation direction.[6] In Fe^{3+} and Fe^{2+} ions, both the magnetic moment and transition dipole strength are large, thereby leading to a high Verdet Constant.[33]

As denoted recently by Nelson et al., C-term MO responses are ideal for applications where minimal optical loss is desired because the peak of the MO response is shifted with respect to the peak of the absorption band and the MO response has a long tail, extending beyond the region of strong absorption.[6] On this basis, we believe that doping with Tb^{3+} leads to an additional strong C-term contribution to the NIR Faraday rotation, originating from its high magnetic moment as well as its 4f-5d allowed transition in the near UV region.[35] The fact that the MO enhancement peaks around 1.12 mol % before it starts decreasing suggests that another competing effect starts to take over at higher doping levels. A likely culprit in this case is the lattice distortion created by the incorporation of larger amounts of Tb^{3+} ions, thereby negatively affecting the overall magnetic ordering of the ions in the magnetite lattice. Previous studies on rare earth ion doped magnetite nanoparticles have observed a similar behavior with respect to the saturation magnetization and attributed it to the increased lattice strain and disorder and the possible formation of secondary phases when the rare-earth doping exceeds the critical solubility limit.[25,26,36,37]

In summary, we report a new strategy to simultaneously enhance the Verdet constant and FOM by doping magnetite nanoparticles with Tb^{3+} ions. At the optimal Tb^{3+} doping density of 1.12 mol %, the PMMA-Fe_3O_4:Tb^{3+} nanocomposite is one of a kind that simultaneously

achieves high Verdet constant of 5.6×10^5 °/T·m and high FOM of 31°/T in the NIR, benefiting all applications in either the power-abundant or the power-starved regimes. Our work demonstrates a new strategy toward engineering high performing MO nanoparticles and paves the way toward their potential in magnetic field sensing and imaging.

Supplementary Material

Refer to Web version on PubMed Central for supplementary material.

ACKNOWLEDGMENTS

We would also like to acknowledge Eric Rappeport for his help in taking the TEM images of the nanoparticles and Conrad Corbella Bagot and Eric Rappeport their insightful discussions on fabrication and experimental procedures.

Funding

National Institute of Biomedical Imaging and Bioengineering REB029541A.

ABBREVIATIONS

MO	Magento-Optic
NIR	Near Infrared
FOM	Figure of Merit
PMMA	Poly(methyl methacrylate)
IVCT	Intervalence charge transfer

REFERENCES

(1). Jacobs SD; Teegarden KJ; Ahrenkiel RK Faraday Rotation Optical Isolator for 106-Mm Radiation. Appl. Opt 1974, 13 (10), 2313. [PubMed: 20134681]

(2). Xia K; Zhao N; Twamley J Detection of a Weak Magnetic Field via Cavity Enhanced Faraday Rotation. Phys. Rev. A 2015, 92 (4), No. 043409.

(3). Carothers KJ; Norwood RA; Pyun J High Verdet Constant Materials for Magneto-Optical Faraday Rotation: A Review. Chem. Mater 2022, 34 (6), 2531–2544.

(4). Vojna D; Slezák O; Lucianetti A; Mocek T Verdet Constant of Magneto-Active Materials Developed for High-Power Faraday Devices. Applied Sciences 2019, 9 (15), 3160.

(5). Piller H Chapter 3 Faraday Rotation. Semiconductors and Semimetals 1972, 8, 103–179.

(6). Nelson Z; Delage-Laurin L; Swager TM ABCs of Faraday Rotation in Organic Materials. J. Am. Chem. Soc 2022, 144 (27), 11912–11926. [PubMed: 35762922]

(7). Slezak O; Yasuhara R; Lucianetti A; Mocek T Wavelength Dependence of Magneto-Optic Properties of Terbium Gallium Garnet Ceramics. Opt Express 2015, 23 (10), 13641. [PubMed: 26074614]

(8). Gao G; Winterstein-Beckmann A; Surzhenko O; Dubs C; Dellith J; Schmidt MA; Wondraczek L Faraday Rotation and Photoluminescence in Heavily Tb3+-Doped GeO2-B2O3-Al2O3-Ga2O3 Glasses for Fiber-Integrated Magneto-Optics. Scientific Reports 2015, 5, 8942. [PubMed: 25754819]

(9). Pavlopoulos NG; Kang KS; Holmen LN; Lyons NP; Akhoundi F; Carothers KJ; Jenkins SL; Lee T; Kochenderfer TM; Phan A; Phan D; Mackay ME; Shim IB; Char K; Peyghambarian N; LaComb LJ; Norwood RA; Pyun J Polymer and Magnetic Nanoparticle Composites with

Tunable Magneto-Optical Activity: Role of Nanoparticle Dispersion for High Verdet Constant Materials. J. Mater. Chem. C Mater 2020, 8 (16), 5417–5425.

(10). Lopez-Santiago A; Gangopadhyay P; Thomas J; Norwood RA; Persoons A; Peyghambarian N Faraday Rotation in Magnetite-Polymethylmethacrylate Core-Shell Nanocomposites with High Optical Quality. Appl. Phys. Lett 2009, 95 (14), 143302.

(11). Ahrenkiel RK; Coburn TJ; Pearlman D; Carnall E; Martin TW; Lyu SL A New Class of Room-Temperature Magneto-Optic Insulators: The Cobalt Ferrites. AIP Conference Proceedings 1975, 24, 186–187.

(12). Lopez-Santiago A; Grant HR; Gangopadhyay P; Voorakaranam R; Norwood RA; Peyghambarian N Cobalt Ferrite Nanoparticles Polymer Composites Based All-Optical Magnetometer. Opt Mater. Express 2012, 2 (7), 978.

(13). Carothers KJ; Lyons NP; Pavlopoulos NG; Kang K-S; Kochenderfer TM; Phan A; Holmen LN; Jenkins SL; Shim IB; Norwood RA; Pyun J Polymer-Coated Magnetic Nanoparticles as Ultrahigh Verdet Constant Materials: Correlation of Nanoparticle Size with Magnetic and Magneto-Optical Properties. Chem. Mater 2021, 33 (13), 5010–5020.

(14). Barnakov YA; Scott BL; Golub V; Kelly L; Reddy V; Stokes KL Spectral Dependence of Faraday Rotation in Magnetite-Polymer Nanocomposites. J. Phys. Chem. Solids 2004, 65 (5), 1005–1010.

(15). Miles A; Gai Y; Gangopadhyay P; Wang X; Norwood RA; Watkins JJ Improving Faraday Rotation Performance with Block Copolymer and FePt Nanoparticle Magneto-Optical Composite. Opt Mater. Express 2017, 7 (6), 2126.

(16). Xu Y; Zhang W; Tian C Recent Advances on Applications of NV – Magnetometry in Condensed Matter Physics. Photonics Res 2023, 11 (3), 393.

(17). Onbasli MC; Beran L; Zahradník M; Kučera M; Antoš R; Mistrík J; Dionne GF; Veis M; Ross CA Optical and Magneto-Optical Behavior of Cerium Yttrium Iron Garnet Thin Films at Wavelengths of 200–1770 Nm. Sci. Rep 2016, 6 (1), 23640. [PubMed: 27025269]

(18). Gyergyek S; Pahovnik D; Žagar E; Mertelj A; Kostanjšek R; Beković M; Jagodič M; Hofmann H; Makovec D Nanocomposites Comprised of Homogeneously Dispersed Magnetic Iron-Oxide Nanoparticles and Poly(Methyl Methacrylate). Beilstein Journal of Nanotechnology 2018, 9 (1), 1613–1622. [PubMed: 29977695]

(19). Jin Y; Kishpaugh D; Liu C; Hajagos TJ; Chen Q; Li L; Chen Y; Pei Q Partial Ligand Exchange as a Critical Approach to the Synthesis of Transparent Ytterbium Fluoride–Polymer Nanocomposite Monoliths for Gamma Ray Scintillation. J. Mater. Chem. C Mater 2016, 4 (16), 3654–3660.

(20). Valiev UV; Gruber JB; Burdick GW; Mukhammadiev AK; Fu D; Pelenovich VO Some Interesting Features of the Tb3+ Magnetooptics in the Paramagnetic Garnets. Opt Mater. (Amst) 2014, 36 (7), 1101–1111.

(21). Rice KP; Russek SE; Geiss RH; Shaw JM; Usselman RJ; Evarts ER; Silva TJ; Nembach HT; Arenholz E; Idzerda YU Temperature-Dependent Structure of Tb-Doped Magnetite Nanoparticles. Appl. Phys. Lett 2015, 106 (6), No. 062409.

(22). De Silva CR; Smith S; Shim I; Pyun J; Gutu T; Jiao J; Zheng Z Lanthanide(III)-Doped Magnetite Nanoparticles. J. Am. Chem. Soc 2009, 131 (18), 6336–6337. [PubMed: 19368388]

(23). Polozhentsev OE; Kubrin SP; Butova VV; Kochkina VK; Soldatov AV; Stashenko VV Structure and Magnetic Properties of Pure and Samarium Doped Magnetite Nanoparticles. Journal of Structural Chemistry 2016, 57 (7), 1459–1468.

(24). Jain R; Luthra V; Gokhale S Dysprosium Doping Induced Correlated Electrical and Optical Behaviour of Magnetite Nanoparticles. AIP Conference Proceedings 2019, 2136, 040002.

(25). Jain R; Luthra V; Gokhale S Probing Influence of Rare Earth Ions (Er3+, Dy3+ and Gd3+) on Structural, Magnetic and Optical Properties of Magnetite Nanoparticles. J. Magn Magn Mater 2018, 456, 179–185.

(26). Nikoforov VN; Oksengendler BL Magnetometric Study of Gadolinium Solubility in Magnetite Nanocrystals. Inorg. Mater 2014, 50 (12), 1222–1225.

(27). Bloemen M; Vandendriessche S; Goovaerts V; Brullot W; Vanbel M; Carron S; Geukens N; Parac-Vogt T; Verbiest T Synthesis and Characterization of Holmium-Doped Iron Oxide Nanoparticles. Materials 2014, 7 (2), 1155–1164. [PubMed: 28788506]

(28). Cheng F; Liao C; Kuang J; Xu Z; Yan C; Chen L; Zhao H; Liu Z Nanostructure Magneto-Optical Thin Films of Rare Earth (RE = Gd,Tb,Dy) Doped Cobalt Spinel by Sol-Gel Synthesis. J. Appl. Phys 1999, 85 (5), 2782–2786.

(29). Kataoka T; Tsukahara Y; Hasegawa Y; Wada Y Size-Controlled Synthesis of Quantum-Sized EuS Nanoparticles and Tuning of Their Faraday Rotation Peak. Chem. Commun 2005, No. 48, 6038.

(30). Royer F; Jamon D; Rousseau JJ; Cabuil V; Zins D; Roux H; Bovier C Experimental Investigation on γ−Fe $_2$ O $_3$ Nanoparticles Faraday Rotation: Particles Size Dependence. European Physical Journal Applied Physics 2003, 22 (2), 83–87.

(31). Lakić M; Andjelković L; Šuljagić M; Vulić P; Perić M; Iskrenović P; Krstić I; Kuraica MM; Nikolić AŚ Optical Evidence of Magnetic Field-Induced Ferrofluid Aggregation: Comparison of Cobalt Ferrite, Magnetite, and Magnesium Ferrite. Opt Mater. (Amst) 2019, 91, 279–285.

(32). Tang J; Myers M; Bosnick KA; Brus LE Magnetite Fe $_3$ O $_4$ Nanocrystals: Spectroscopic Observation of Aqueous Oxidation Kinetics. J. Phys. Chem. B 2003, 107 (30), 7501–7506.

(33). Fontijn WFJ; van der Zaag PJ; Feiner LF; Metselaar R; Devillers MAC A Consistent Interpretation of the Magneto-Optical Spectra of Spinel Type Ferrites (Invited). J. Appl. Phys 1999, 85 (8), 5100–5105.

(34). Demesh M; Gorbachenya K; Kisel V; Volkova E; Maltsev V; Koporulina E; Dunina E; Kornienko A; Fomicheva L; Kuleshov N Transitions Intensities and Cross-Sections of Tb 3+ Ions in YAl 3 (BO 3) 4 Crystal. OSA Contin 2021, 4 (3), 822.

(35). Dorenbos P The 5d Level Positions of the Trivalent Lanthanides in Inorganic Compounds. J. Lumin 2000, 91 (3–4), 155–176.

(36). Jain R; Luthra V; Gokhale S Dysprosium Doping Induced Shape and Magnetic Anisotropy of Fe3−Dy O4 (X = 0.01–0.1) Nanoparticles. J. Magn Magn Mater 2016, 414, 111–115.

(37). Obaidat IM; Mohite V; Issa B; Tit N; Haik Y Predicting a Major Role of Surface Spins in the Magnetic Properties of Ferrite Nanoparticles. Crystal Research and Technology 2009, 44 (5), 489–494.

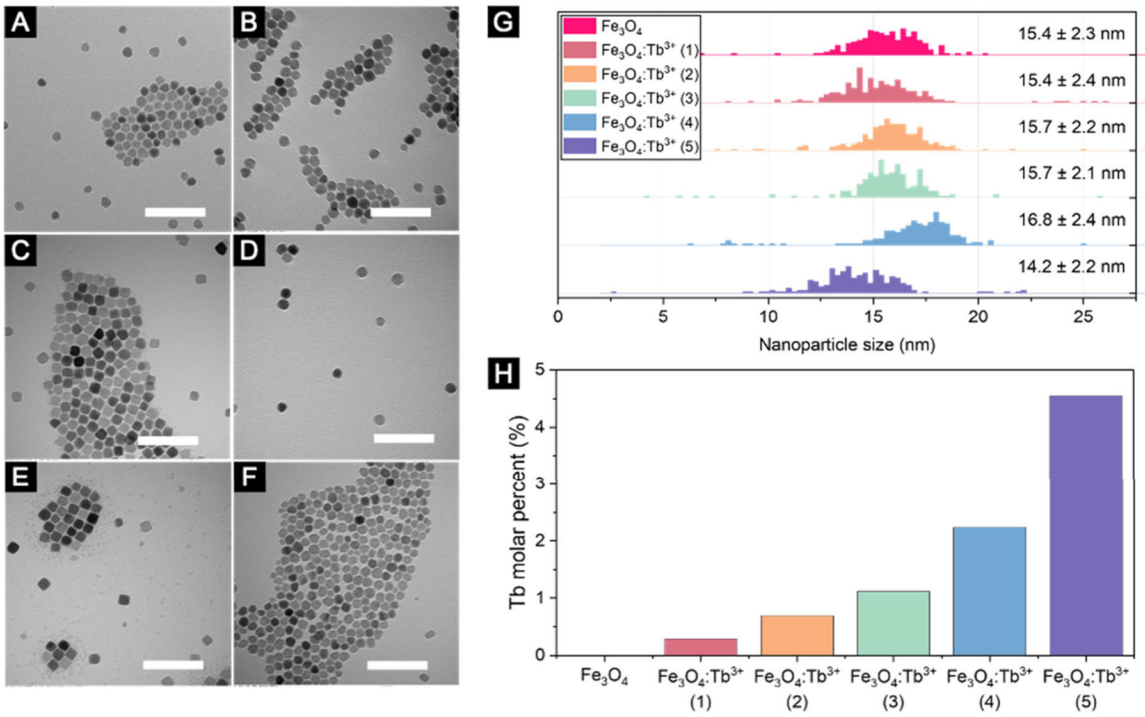

Figure 1.

Representative TEM images of (A) undoped and (B–F) Tb^{3+} doped magnetite nanoparticles after synthesis. Scale bar is 100 nm. (G) Size distribution of the nanoparticles as calculated from TEM images using the software package ImageJ. (H) Tb^{3+} doping density in the nanoparticles as characterized by ICP-MS analysis.

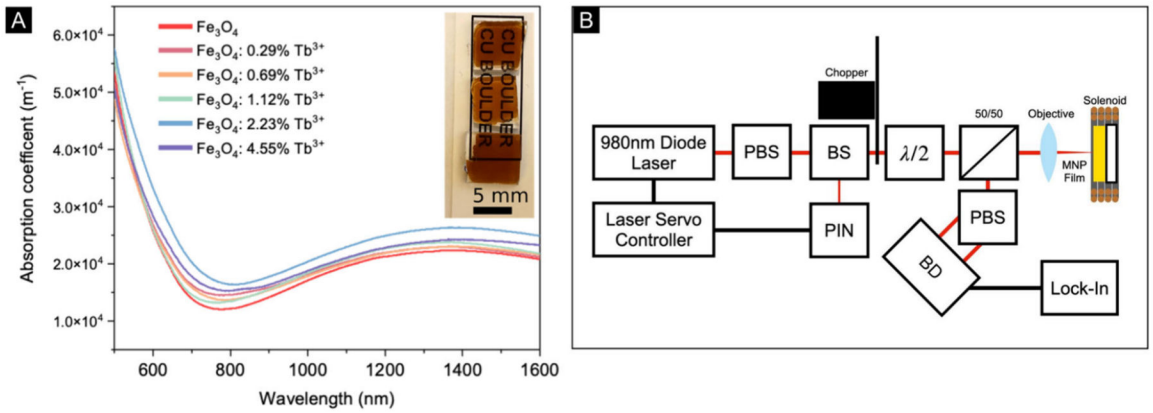

Figure 2.

(A) VIS–NIR absorption coefficient of the PMMA-Fe3O4:Tb^{3+} nanocomposite. Inset: optical image of three nanocomposite films with different Tb^{3+} doping densities of 0.29% (top), 1.12% (middle), and 4.55% (bottom). (B) System schematic, PBS: Polarizing beam splitter, $\lambda/2$: Half waveplate, BS: Beams sampler, PIN: Photodetector, BD: Balanced detector.

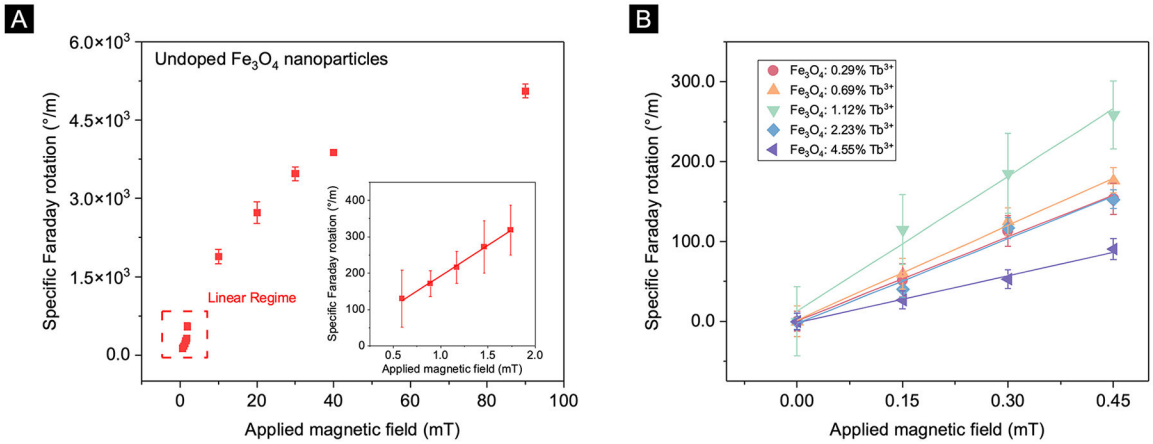

Figure 3.

(A) Specific Faraday rotation of undoped nanoparticle thin films demonstrating saturation above 10 mT, inset demonstrating the linear regime of nanoparticles. (B) Verdet Constant measurements of all fabricated thin films in the linear region. The solid lines are the linear fits of the specific Faraday rotation as a function of the applied DC magnetic field.

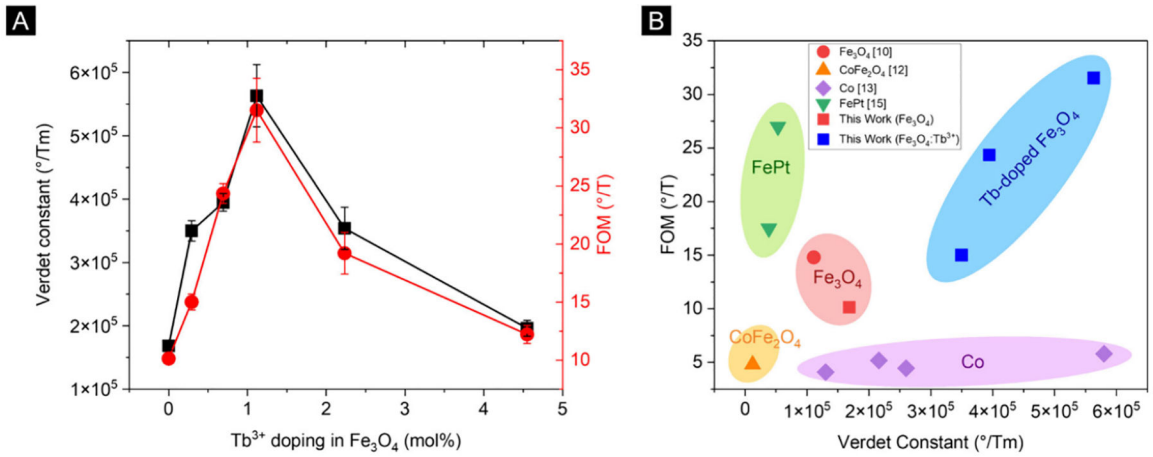

Figure 4.

(A) Verdet constant and FOM as a function of the Tb^{3+} doping density. Positive sign indicates clockwise polarization rotation of light in an antiparallel magnetic field. (B) Comparison against other room temperature MO polymer nanocomposite in the NIR (800–1300 nm).[9,11,12,14]